ORIGINAL ARTICLE

Differential targets of CpG island hypermethylation in primary and metastatic head and neck squamous cell carcinoma (HNSCC)

D J Smiraglia, L T Smith, J C Lang, L J Rush, Z Dai, D E Schuller, C Plass

J Med Genet 2003;**40**:25–33

See end of article for authors' affiliations

Correspondence to: Dr D J Smiraglia, The Ohio State University, Department of Molecular Virology, Immunology and Medical Genetics, Division of Human Cancer Genetics, 420 West 12th Avenue, Medical Research Facility, Room 470A, Columbus, OH 43210, USA; Smiraglia.1@osu.edu

Revised version received 30 August 2002
Accepted for publication 1 September 2002

Head and neck squamous cell carcinomas (HNSCC) often metastasise to the cervical lymph nodes. It is known for HNSCC as well as other cancers that progression from normal tissue to primary tumour and finally to metastatic tumour is characterised by an accumulation of genetic mutations. DNA methylation, an epigenetic modification, can result in loss of gene function in cancer, similar to genetic mutations such as deletions and point mutations. We have investigated the DNA methylation phenotypes of both primary HNSCC and metastatic tumours from 13 patients using restriction landmark genomic scanning (RLGS). With this technique, we were able to assess the methylation status of an average of nearly 1300 CpG islands for each tumour. We observed that the number of CpG islands hypermethylated in metastatic tumours is significantly greater than what is found in the primary tumours overall, but not in every patient. Interestingly, the data also clearly show that many loci methylated in a patient's primary tumour are no longer methylated in the metastatic tumour of the same patient. Thus, even though metastatic HNSCC methylate a greater proportion of CpG islands than do the primary tumours, they do so at different subsets of loci. These data show an unanticipated variability in the methylation state of loci in primary and metastatic HNSCCs within the same patient. We discuss two possible explanations for how different epigenetic events might arise between the primary tumour and the metastatic tumour of a person.

Head and neck squamous cell carcinomas (HNSCC) of the oral cavity, pharynx, and larynx occur at a rate of approximately 500 000 new cases per year world wide.[1] The overall five year survival rate for patients without clinically evident cervical lymph node metastases is 85% with little variation dependent upon tumour staging. However, patients with microscopic lymph node metastases have a survival rate of 54%. It has been estimated that 20-50% of patients without clinically evident cervical lymph node metastases do in fact have microscopic metastases and therefore a poor prognosis.[2]

It is widely accepted that cancer results from a multistep process in which a series of genetic "hits" are required to allow cells to progress through hyperplasia, dysplasia, carcinoma in situ (CIS), invasive tumour, and metastatic tumour. The genetic progression model for colorectal tumorigenesis serves as a template for many other cancers.[3] It is clear that the accumulation of genetic damage correlates with the progression of cells towards metastasis. Califano *et al*[4] proposed a similar model of accumulation of genetic changes in HNSCC, where events such as loss of chromosome 9p occur frequently and early, while loss of 4q occurs late in tumour progression.

Little is known about the specific gene defects that are associated with HNSCC progression. The most common type of molecular defect is unbalanced translocations causing deletions.[5 6] Loss of heterozygosity (LOH) of 18q[7] and of 13q14.3[8] has been correlated with HNSCC progression and metastasis. In addition, overexpression of *ETS-1*, which is not expressed in normal epithelium, has been correlated with stage III and stage IV primary tumours, as well as metastatic involvement of the cervical lymph nodes.[9] Thus, evidence is accumulating that, as in other tumour types, it is possible to identify distinct molecular defects associated with specific stages of the development of HNSCC.

DNA hypermethylation of CpG islands in the promoters of genes is a well studied epigenetic alteration of the genome that is known to play a significant role in cancer.[10–15] The effect of such promoter hypermethylation can be analogous to genetic loss of function mutations such as point mutations and deletions. DNA hypermethylation of a promoter is thought to transcriptionally suppress the gene through the recruitment of chromatin remodelling complexes.[16–19] Thus, promoter hypermethylation of a tumour suppressor gene is one way in which a cell may acquire one or more of the "hits" that must accumulate in order to progress towards malignancy and/or metastasis.

The $p16^{INK4a}$ (*p16*) gene is located on chromosome 9p21 in a region that is lost frequently and early in HNSCC.[4 20] Genomic analysis of the *p16* locus in tumours lacking the p16 protein showed that 67% had a homozygous deletion of the *p16* locus, and 21% had hypermethylation of the *p16* promoter. In a more recent study of 14 HNSCC cell lines derived from both primary and metastatic tumours of the oral cavity, there was no wild type *p16* expression found. Analysis of the locus determined that 21% had homozygous deletions, 29% had exonic mutations, 14% had intronic mutations, and 29% showed hypermethylation of the *p16* promoter.[21]

Investigation of genes known to exhibit promoter hypermethylation in other cancers has shown that promoter hypermethylation does play a role in HNSCC.[20 22–27] Interestingly, in a study of four known genes, no correlation between overall hypermethylation and clinicopathological factors could be made. However, hypermethylation of one gene, *DAP-kinase*, was positively correlated with stage III-IV tumours and nodal involvement.[27] These observations raise the following questions. To what degree does CpG island hypermethylation contribute to the genomic abnormalities in HNSCC, and do hypermethylation events accumulate as cells progress towards metastasis?

Here we report the assessment of the hypermethylation phenotypes of 13 primary HNSCCs and cervical lymph node metastases from the same 13 patients. We have used the

restriction landmark genomic scanning (RLGS) technique to assess the methylation status of an average of 1293 *Not*I sites in normal adjacent tissue, primary tumour, and cervical lymph node metastasis from all 13 patients. Although quantitatively we detect a higher proportion of RLGS fragments methylated in the metastatic tumours, this is not simply an accumulation of methylation events since many events found in the primary tumour are not found in the metastatic tumour of the same patient.

MATERIALS AND METHODS

Tissue collection

Primary head and neck squamous cell carcinomas of the oral cavity, larynx, and pharynx, and metastases to the cervical lymph nodes were obtained from the Cooperative Human Tissue Network. All patients were operated on at The Ohio State University and included 11 males and two females ranging from 42 to 77 years of age. The 13 patients' sample sets were chosen only where the metastatic lymph node contained grossly visible tumour. All normal specimens were harvested from morphologically normal appearing tissue located at least 3 cm from the tumour margin and were used as the normal control tissue for comparisons with the tumour tissues. Pathological evaluation of the normal, primary tumour, and metastatic tissues was performed. All tissues were snap frozen in liquid nitrogen and stored at –80°C before DNA isolation. All tissues were collected under a protocol approved by the Institutional Review Board of The Ohio State University.

RLGS

RLGS gels were run as previously described.[13 28 29] For each patient set, the normal profile was compared to the primary tumour profile and to the metastatic tumour profile. In each comparison, RLGS fragments present in the normal profile and absent or greatly reduced in intensity (visual inspection) in one or both tumour profiles from the same patient were scored as methylation events. We have previously determined by comparing quantitative Southern blot analysis with RLGS profile analysis that we can reliably detect loss of spot intensity equal to 30-40% methylation. Such loss events were scored equally as methylation events regardless of whether the loss appeared to be closer to 40% or 100%. Therefore, despite the presence of normal contaminating tissue we are still able to detect methylation in the malignant cells as long as the majority of the tissue used for DNA isolation is malignant. Thus, methylation of a locus in 80% of malignant cells within a tissue with 30% normal cells is well within our detection capabilities. In addition, we and others have previously shown that RLGS spot loss equates with methylation.[10 13 30] RLGS fragments were identified by a coordinate naming system previously described.[13] Polymorphic fragments not found in the RLGS master profile used for naming are uniquely named by their section, followed by "XHN" and an arbitrary number (for example, 2DXHN47 indicating section 2D and fragment XHN47).

RLGS fragment cloning

RLGS fragments were cloned using the *Not*I/*Eco*RV boundary library mixing gels as previously described.[31] Single pass sequencing was performed from the *Not*I end of the clone and used for database searches at NCBI. CpG island characteristics were determined using a CpG island prediction tool at the WebGene web site (http://www.itba.mi.cnr.it/webgene/). All sequencing was performed at the Genotyping and Sequencing Unit (GSU) at The Ohio State University, Division of Human Cancer Genetics.

Bisulphite treatment, PCR, and sequencing

Bisulphite treatment of DNA and subsequent PCR was performed as described by Herman *et al*[32] with the exceptions that the DNA purification before and after alkali desulphonation was done using the Qiagen gel extraction kit (Qiagen). Bisulphite treated DNA was used as template in PCR reactions set up as previously described.[32] The PCR reactions were run for 35 cycles. The primers used to amplify the promoter region of the *formin 2* like gene are forward 5′ . . .TTGGAGTTTTGGTGAGTAGGG . . .3′, and reverse 5′ . . .CCCAAAAATATAAAAACCACAAAAA . . .3′ with an annealing temperature of 59°C. The bisulphite converted sequence of RLGS fragment 2C54 was amplified using the primers forward 5′ . . .GAGGAGGAGAAGGAGGAGGA . . .3′, and reverse 5′ . . .CRACRCCRATATCACATTTA . . .3′ with an annealing temperature of 48°C. Methylation sensitive PCR (MS-PCR) for *p16* was performed as previously described using the p16M2 and p16U2 primers.[32] Bisulphite sequencing primers for *p16* were designed just flanking these MS-PCR primers: forward 5′ . . .GGAGGGGTTGGTTGGTTATT . . .3′, and reverse 5′ . . .CAAACCCTCTACCCACCTAAA . . .3′ with an annealing temperature of 61°C. The PCR products were gel purified using the Qiagen gel extraction kit, and cloned using the TA Cloning kit (Invitrogen). Individual clones were sequenced using the M13F primer.

RT-PCR and sequencing

Total RNA was extracted from tissue using a modification of our previously described method.[33] Briefly, specimens were placed in individual plastic bags partly immersed in liquid nitrogen. The bags were resistant to cracking under low temperature exposure. Frozen tissue was crushed by repetitive strikes with a hammer and dissolved in TRIzol reagent (Invitrogen Life Technologies, Carlsbad, CA) by direct addition to the bag. Specimens were then transferred to centrifuge tubes, followed by freeze-thawing, and debris removed by brief centrifugation. RNA was then extracted according to the manufacturer's protocol; 1.0 µg of total RNA was used for first strand cDNA synthesis in a total volume of 25 µl and reactions otherwise performed according to the manufacturer's instructions (ProSTAR, Stratagene, La Jolla, CA). PCR amplification was performed using the Advantage-GC PCR kit (CLONTECH, Palo Alto, CA). Separate reactions were performed for each primer pair with the following reaction conditions: 96°C for one minute followed by 94°C for 30 seconds, 65°C for 30 seconds, 72°C for one minute for 35 cycles (*p16*), or 33 cycles (*p14*) and a final five minute extension at 72°C. PCR samples were then run through 2% agarose gels and the presence of amplified product and correct product size verified by ethidium bromide fluorescence in the presence of 100 bp size markers (Gibco BRL, Gaithersburg, MD). Primers were designed by computer analysis (Oligo 4.0, NBI, Hamel, MN) of available DNA sequence for each gene and are intron spanning, precluding PCR amplification of any residual DNA present in RNA samples. Optimum cycle number for PCR amplification was predetermined for each primer set using a mixture of RT reactions from 12 random tumour samples (data not shown). This step is necessary to ensure that PCR amplification remains in the linear range and that production of PCR product does not plateau. Primers used in PCR reactions comprise p16: p16-15, 5′-GGAGAGGGGGAGAGCAGGCAGC-3′ and p16-14, 5′-TGGCCCTG TAGGACCTTCGGTGAC-3′, $p14^{ARF}$: P14-1, 5′-CGCGCCTGCGGGGCGGA-3′.

RESULTS

Quantification of hypermethylation phenotypes in primary and metastatic HNSCCs

RLGS profiles were prepared from the DNA of primary tumour tissue, normal adjacent tissue, and cervical lymph node metastatic tissue from 13 HNSCC patients. For each patient, the normal tissue profile was compared to both the primary tumour profile and the metastatic tumour profile and RLGS

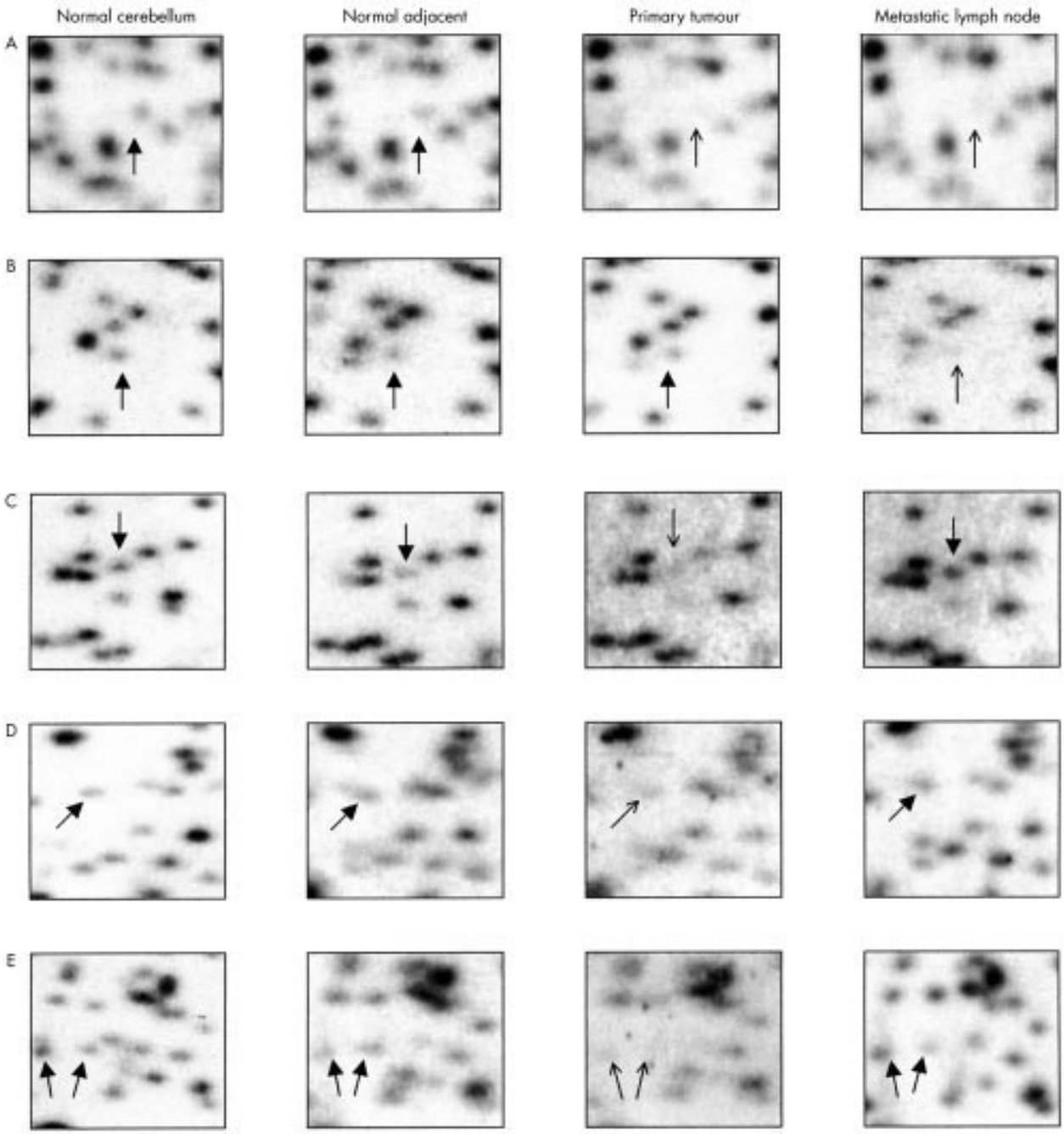

Figure 1 Representative examples of RLGS analysis. Sections of RLGS profiles are shown from normal cerebellum obtained from a non-cancer patient at necropsy, as well as HNSCC patient normal adjacent tissues, primary tumour tissues, and metastatic tumour tissues. The solid arrowheads indicate normal presence of the RLGS fragment, and the open arrowheads indicate reduced RLGS fragment intensity. (A) Profiles showing the RLGS fragment 5E25 lost in both the primary and metastatic tumours of patient 32. (B) Profiles showing the RLGS fragment 4E1 lost only in the metastatic tumour of patient 7. (C) Profiles showing the RLGS fragment 2D45 lost in the primary tumour, but not the metastatic tumour of patient 8. (D) Profiles showing the RLGS fragment 2C61 lost in the primary tumour, but not the metastatic tumour of patient 4. (E) Profiles showing the RLGS fragments 4E24 and 4F22 lost in the primary tumour, but not the metastatic tumour of patient 4.

fragments were scored for presence or absence in the tumour profiles (see Materials and methods). A total of 33 617 RLGS fragments were analysed in the set of 26 tumours for a mean of 1293/tumour profile with a range of 747-2126. Fig 1 shows portions of RLGS profiles representative of this data set. Note that although the overall intensity varies from gel to gel, spot loss is determined by loss of intensity relative to the surrounding spots. In addition, the fact that spot loss is not 100% in most cases may be explained by partial methylation and/or normal contaminating tissue that is not methylated. In all cases, the non-cancer related normal cerebellum profile shows the normal intensity of the spots, while in some instances the normal adjacent tissue shows slightly reduced intensity (fig 1A, C). Methylation in both the primary tumour and the metastatic tumour was often observed (fig 1A), as was methylation in the metastatic tumour only (fig 1B). More surprisingly, there were many instances where methylation was detected in a patient's primary tumour, but not in the metastatic tumour from the same patient. Three such examples are shown in fig 1C, D, and E.

We found that 104 RLGS fragments present in at least one patient's normal tissue profile were absent from either one or

Table 1 Patient and RLGS analysis data for 13 HNSCC patients

Patient	Age (y)	Sex	Race	Tissue	% of analyed loci methylated		*Primary only	†Metastatic only	‡Both	§NA	¶% lost in primary but not metastasis
					Primary	Metastatic					
2	44	M	Bl	Tongue	2.1	1.9	6	12	16	0	27
4	56	M	Wh	Pharynx	1.2	0.57	13	6	1	0	93
7	52	M	Wh	Pharynx	1.3	1.2	14	14	8	0	64
8	46	M	Wh	Tonsil	0.76	0.67	11	8	3	0	79
11	67	M	Wh	Tonsil	0.09	0.36	1	5	1	0	50
12	65	F	Wh	Tonsil	1.4	1.6	5	16	8	1	38
14	65	M	Wh	Larynx	0.74	1.4	6	16	2	2	75
15	77	F	Wh	Tonsil	0.90	3.3	9	27	1	0	90
16	59	M	Wh	Tongue	0.74	1.9	2	12	4	0	33
23	42	M	Wh	Pharynx	2.0	3.1	8	14	7	3	53
28	48	M	Wh	Tongue	0.46	1.2	4	15	2	0	67
29	62	M	Wh	Tongue	1.2	1.9	2	11	10	0	17
32	65	M	Wh	Pharynx	1.3	1.8	12	17	7	1	63
Ave					**0.99	**1.47					58

*Number of loci methylated in the primary tumour, but not the metastatic tumour.
†Number of loci methylated in the metastatic tumour, but not the primary tumour.
‡Number of loci methylated in both the primary and metastatic tumours.
§Number of loci that were methylated in one tumour, but unable to be analysed in the other tumour RLGS profile.
¶Number of loci methylated in the primary only divided by the number of loci methylated in primary only plus the number methylated in both primary and metastasis.
**An unpaired Z test test using the normal approximation to the binomial distribution to compare the frequencies of methylation between primary tumours and metastatic tumours indicates significantly more methylation in the metastatic tumours as a group ($p<<0.001$).

both of that patient's tumour profiles (table 1). These RLGS fragment losses are indicative of methylation of those loci.[13] Within each patient set, we have identified loci that are methylated in the primary tumour only, the metastatic tumour only, or in both (table 1, fig 1). The percentage of RLGS fragment methylation ranges from 0.09% to 2.10% in primary tumours and from 0.36% to 3.30% in metastatic tumours. The frequencies of locus methylation are similar in primary tumours and metastatic tumours; 23 of the 67 loci methylated in primary tumours (34%) are methylated in more than 30% of the patients and 34 of the 89 loci methylated in metastatic tumours (38%) are methylated in more than 30% of the patients. The differences in the frequency distributions of locus methylation are not statistically significant (Komogorov-Smirnov goodness of fit test, $p=0.23$).

The degree of hypermethylation in primary and metastatic tumours is compared in table 1. The combined data from all 13 patients indicate that 0.99% of the RLGS fragments are methylated in the primary tumours, while 1.47% are methylated in metastatic lymph nodes. A total of 167 methylation events out of 16 868 data points were detected in primary tumours, and 246 methylation events out of 16 749 data points were detected in metastatic tumours. An unpaired Z test using the normal approximation to the binomial distribution to compare the frequencies of methylation between primary tumours and metastatic tumours gives a Z statistic of –3315.4, indicating significantly more methylation in the metastatic tumours ($p<<0.001$).

Primary and metastatic tumours show methylation of different loci

Additional information can be gleaned by studying the distribution of locus hypermethylation in each individual patient set (table 1). With the exceptions of patients 2 and 29, the degree of overlap between loci methylated in the primary tumour and the metastatic tumour is surprisingly small. Patients 4, 7, 8, and 32 exhibit more than 10 loci that are methylated in their primary tumours, but are no longer methylated in their metastatic tumours. These observations cannot be explained by contaminating normal tissue masking our ability to detect methylation since numerous other loci are methylated in these metastatic tumours. The percentage of loci methylated in the primary tumour of a patient, but not in the metastatic tumour from the same patient range from 17% to 93% (table 1). These data indicate that the group of loci that become hypermethylated in HNSCC tumours may differ significantly between the primary tumour and metastatic tumour of an individual person and, furthermore, that this difference is highly patient specific.

One hundred and four methylated loci have been identified in this patient set. By combining the data from all 13 patient sets, we are able to look for trends in the methylation state of specific loci. Eight loci are methylated exclusively in primary tumours, 17 in metastatic tumours, and 79 in both the primary and metastatic tumours; 88 of the 104 methylated loci in this data set are lost in more than one tumour. The distribution of the methylation events found in the 26 tumour samples is shown in fig 2 for these 88 loci. There are 86 instances where a locus is methylated only in a patient's primary tumour, 170 only in a patient's metastatic tumour, and 73 in both the primary and metastatic tumours of an individual patient.

Cloning and characterisation of targets of hypermethylation

Fifteen hypermethylated loci were readily clonable using the *Not*I/*Eco*RV boundary library and mixing gel cloning techniques previously described.[31 34] All 15 were confirmed by mixing gel analysis. Chromosomal location, CpG island traits, and the genomic context of these 15 loci are shown in table 2. All 15 loci fall within CpG islands.[35] Homologies to known genes were identified for six loci, to ESTs for six, and to a pseudogene for one locus. For all six known genes, the CpG island from which the RLGS fragment arises is found in the promoter region and 5′ end of the gene.

Methylation differences between primary and metastatic tumours are confirmed by bisulphite sequencing

There were 93 instances where an RLGS fragment was methylated in the primary tumour, but was not methylated in the metastatic tumour from the same patient (table 1, fig 1C, D, E). To investigate this surprising finding in more detail, an RLGS fragment (2C54) and a tumour suppressor gene previously identified as a target of hypermethylation in HNSCC (*p16*) were further analysed. RLGS profile analysis identified fragment 2C54 as methylated in the primary tumour of patient 23 but not the metastatic tumour.

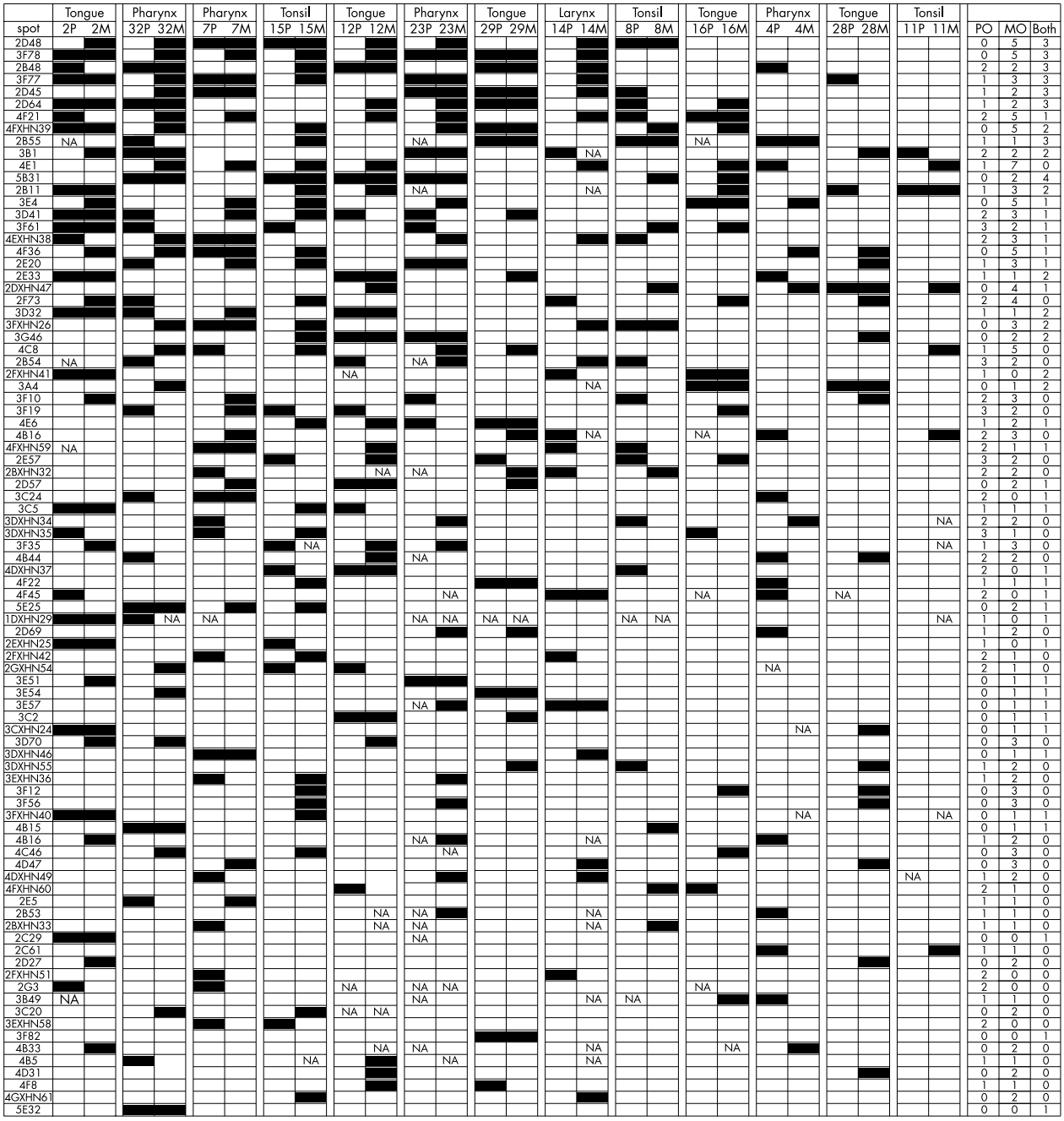

Figure 2 Distribution of methylated loci by patient. Black indicates methylation. White indicates lack of methylation. NA indicates that the fragment was not analysable. P indicates primary tumour. M indicates metastatic tumour. PO indicates the number of patients where loss was in the primary tumour only. MO indicates metastatic tumour only. Both indicates where loss was in both.

Bisulphite sequencing primers were designed to amplify a region within the 2C54 CpG island containing 49 CpG dinucleotides. Fifteen normal, 17 primary tumour, and 24 metastatic tumour clones were sequenced from patient 23. More than twice as much methylation was detected in the primary tumour clones as compared to the metastatic tumour clones. The proportion of clones showing methylation was calculated for each CpG dinucleotide and is plotted in fig 3. The proportion of methylated clones is greatest in the primary tumour throughout the entire set of 49 CpGs studied. The level of methylation detected in the normal tissue and the metastatic tissue overlaps considerably. It is important to note that these data represent a relative quantification, not an absolute quantification. Owing to the previously reported possibility for PCR bias in bisulphite sequencing, we cannot use this method for absolute quantification.[36] The low absolute level of methylation detected here is likely to be a reflection of the relative difficulty of amplifying the methylated product, since it contains up to 49 CpGs within 332 bp.

p16 study provides independent confirmation of methylation unique to a patient's primary tumour

The previous data have shown the phenomenon of methylation present in the primary tumour, but no longer present in the metastatic tumour of the same patient at anonymous RLGS loci. In order to understand better the biological significance of this phenomenon, we looked to see if we could find it in a well characterised tumour suppressor gene whose loss of function has been clearly shown to have biological significance. The *p16* gene promoter has been previously identified as

Table 2 RLGS fragment sequence characteristics

RLGS fragment	Chr location	CpG island traits			Genomic context	Class of methylation
		Size (bp)	%GC	CpG:GpC		
2B53	2q36-q37	1461	65	0.93	5′end/exon 1 of nucleolin gene	Both
2C59	19q13.2	1274	56	0.78	5′end/exon 1 of HSPC059 protein	Primary only
5E25	1q44	2033	70	0.73	5′end/exon 1 of formin-2 like gene	Both
3G46	11q23	1079	55	0.65	5′end/exon 1 of GlcNac-1-P transferase gene	Both
2C54	2q35	1860	68	0.86	5′end/exon 1 of cullin3 gene	Primary only
3E4	11q14	2322	67	0.83	5′end of α1,3 fucosyltransferace gene	Both
3F82	16p11.2	1422	67	0.86	CSDAP1 pseudogene 1	Both
2C29	6q21	885	55	0.75	EST accession No AL516185	Both
3E50	16p13.3	1479	66	0.75	EST accession No BE735354	Primary only
4B44	3q21	653	72	0.77	EST accession No AW294737	Both
4F22	3p25-p26	734	67	0.71	EST accession No AA338277	Both
2D27	4q33-q34	1030	69	0.84	EST accession No BF961384	Metastatic only
3C5	16q12.1	2153	73	0.88	EST accession No AV720746	Both
2D48	7p21	890	60	0.74	No known gene homology	Both
3E57	5	1025	60	0.69	No known gene homology	Both

a target of CpG island hypermethylation in HNSCC and this methylation has been correlated with silencing of the gene. Methylation specific PCR (MS-PCR) was performed for the *p16* promoter as previously described[32] in a set of nine primary and metastatic tumours. Of the nine patients studied in fig 4A, only patient 4's primary tumour showed methylation. No methylation is detected in the metastatic tumour from patient 4; however, the presence of the unmethylated *p16* band indicates that the locus has not been homozygously deleted. The MS-PCR result was confirmed by bisulphite sequencing of 10 clones each for normal adjacent, primary tumour, and metastatic tumour DNA from patient 4 using primers designed to flank the region amplified by MS-PCR. The primary tumour DNA showed heavy methylation of approximately half the clones, while the metastatic tumour showed almost no methylation (fig 4B). Methylation of multiple other loci, as detected by RLGS analysis of the metastatic tumour from patient 4, shows that the ability to detect methylation in this tumour is not masked by contaminating normal tissue.

RT-PCR from RNA obtained from the primary and metastatic tumours from patient 4 showed low expression from the primary tumour where methylation was detected, but high expression from the metastatic tumour where no methylation was detected (fig 4C). The primers used for the *p16* RT-PCR reaction fall in exon 1 of the *p16* transcript and exon 2 shared by both the *p16* and $p14^{ARF}$ (*p14*) transcript. Direct sequencing of the RT-PCR product (the entire *p16* transcript) showed that the transcript expressed in the metastatic tumour has a 17 bp deletion early in exon 2 (nucleotide 219 of the *p16* mRNA), resulting in a frameshift (fig 4D). The frameshift occurs after amino acid

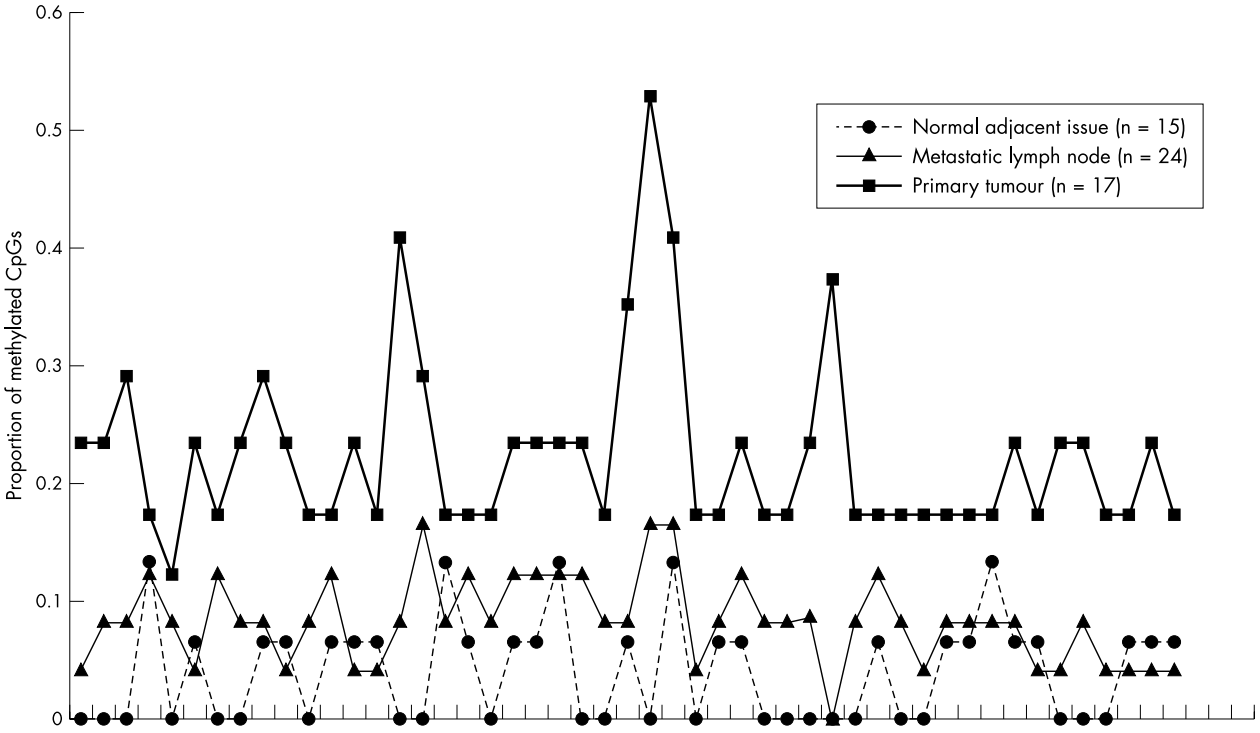

Figure 3 Bisulphite sequencing of RLGS fragment 2C54. After bisulphite PCR of 2C54 from patient 23's HNSCC DNA, 15 normal adjacent tissue clones, 17 primary tumour clones, and 24 metastatic lymph node clones were sequenced. The data are presented as the proportion of CpGs methylated per group of clones for each of 49 CpG dinucleotides sequenced from the 332 bp cloned products. The proportions were calculated by dividing the number of methylated CpGs by the number of clones sequenced from that tissue. The proportion of methylated CpGs is represented on the Y axis, and each of 49 CpGs is represented on the X axis.

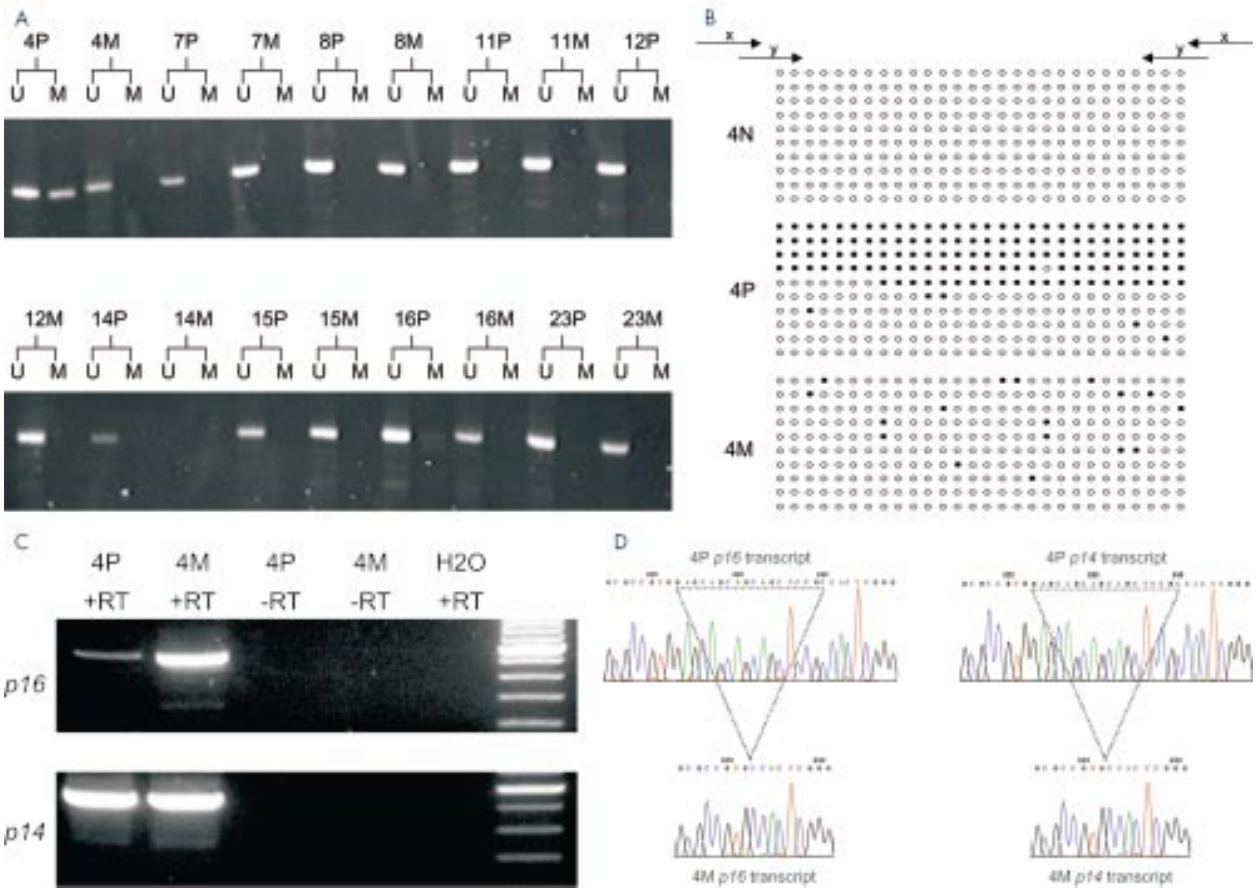

Figure 4 *p16* and *p14* studies. (A) MS-PCR analysis of the *p16* gene promoter on a set of nine pairs of HNSCC DNAs. For each DNA, a separate PCR reaction was run and loaded on a polyacrylamide gel for the unmethylated specific primers (U) and the methylated specific primers (M), as indicated above each lane. The patient numbers are indicated. P, primary tumours; M, metastatic lymph node. (B) "Beads on a string" diagrams indicating the multiple clones sequenced from bisulphite PCR of the *p16* promoter. The arrows indicate primer sets X and Y. The Y primer set indicates the position of the primers used for MS-PCR analysis in (A). The X primer set indicates the position of the primers used for bisulphite PCR. Each bead represents one of 28 CpG dinucleotides analysed with primer set X. Open beads indicate non-methylated CpGs, while closed beads indicate methylated CpGs. Each horizontally arranged string of beads indicates a single sequenced clone. Ten clones each were sequenced from patient 4's normal adjacent tissue, primary tumour, and metastatic lymph node DNAs. N, normal adjacent tissue; P, primary tumours; M, metastatic lymph node. (C) RT-PCR was performed using primers specific to the *p16* and *p14* transcripts on RNA obtained from patient 4's primary tumour and metastatic tumour. The product sizes are 580 bp and 577 bp, respectively. (D) Chromatograms from each of the four RT-PCR products shown in (C). RT-PCR products were gel purified and directly sequenced.

60 and produces a nonsense mutation with a stop codon at amino acid 112. The low level transcript detected in the primary tumour has no mutation.

The transcript detected in the primary tumour may arise from contaminating normal cells, and so to determine if the 17 bp deletion is present in the primary tumour cells the *p14* transcript was studied. RT-PCR was performed on the same samples using a primer specific to the *p14* exon 1, and the same second primer in the shared exon 2 that was used for *p16* RT-PCR. The *p14* transcript is equally expressed in both the primary and the metastatic tumours of patient 4 (fig 4C). Furthermore, direct sequencing of the RT-PCR product shows that, just as with the *p16* transcript, the metastatic tumour has a 17 bp deletion while the primary tumour transcript has no mutation. These results confirm that in patient 4's primary tumour there is methylation of *p16*, but no mutation, whereas in the metastatic tumour from the same patient, there is mutation of *p16* but no methylation. Important to the biology of the tumours, however, both genomic alterations lead to loss of function of the p16 protein.

DISCUSSION

A crucial point in our understanding of cancer biology is that neoplastic cells evolve from the accumulation of genetic changes that give the cells a growth or survival advantage.[3] These genetic changes tend to accumulate in a loose order. For instance, loss of chromosome 9p is a common and early change (often in hyperplasia) in the development of HNSCC, while loss of chromosome 4q is found late (often in CIS and invasive tumour) in HNSCC.[4 20] It seems reasonable to predict that epigenetic changes such as CpG island hypermethylation may also accumulate in a similar manner. To address this idea experimentally, we have used restriction landmark genomic scanning (RLGS) to study the hypermethylation phenotypes in 13 HNSCC patients, comparing the RLGS profiles from their primary tumours and cervical lymph node metastases to their normal adjacent tissue profiles. CpG island hypermethylation is generally thought to result in loss of function of the gene involved owing to suppression of transcription. This is analogous to other loss of function mutations such as deletions and point mutations. Deletions resulting from unbalanced translocations are the most common type of mutation in HNSCC. Nevertheless, it is clear from the data presented in this article, as well as the data of others, that the mutation spectrum in HNSCC also includes CpG island hypermethylation. We found that in the overall data set there is a small but significant increase in the degree of CpG island hypermethylation in metastatic tumours compared to the primary tumours. Importantly, however, we also found that the hypermethylated

loci in primary tumours and metastatic tumours can vary tremendously within a single patient. Thus, even though there tends to be more methylation in any one patient's metastatic tumour, this is not simply the result of an accumulation of additional methylation events, since many found in the primary tumour are no longer found in the metastatic tumour.

The percentage of specific loci that are methylated in the primary tumour of a patient, but not in the metastatic tumour from the same patient varies widely from 17% in patient 29, to 93% in patient 4, with an average of 58% (table 1). This indicates that there is not an accumulation of epigenetic changes in the metastatic tumours, but instead a different set of changes with only a portion of those found in the primary tumour retained in the metastatic tumour. This is reinforced by the bisulphite sequencing data of RLGS fragment 2C54 and the *p16* promoter. Furthermore, the finding of very low *p16* expression in the methylated primary tumour, but high expression in the unmethylated metastatic tumour, and that the metastatic tumour harbours a genetic mutation in *p16* while the primary tumour does not, offers some insight on how to explain these findings.

One interpretation of these data would be to suggest that there is substantial epigenetic heterogeneity within the primary tumours. We would then predict that hypermethylation events present in both the primary and metastatic tumours are from events that were present very early in the development of the primary tumour. Further evolution of the tumour may proceed differently in various regions, either by random chance or by selection because of different microenvironments. This may result in the formation of many unique subpopulations with regard to methylation within the primary tumour. Since our sensitivity with RLGS is limited to reliably detecting 30% hypermethylation of a locus, the hypermethylation events we have detected in primary tumours are likely to be present in most subpopulations of cells within the tumour. If one of the minor subpopulations of cells with differential hypermethylation events acquires characteristics advantageous to metastatic spread, then the hypermethylation we detect in the metastatic tumour would be different from what is detected in the primary tumour. The differential methylation events may or may not directly contribute to the cells' propensity for metastasis.

The fact that patient 4's primary and metastatic tumours have found different ways to inactivate *p16* function fits well within this interpretation. Perhaps because of a field effect, multiple initiated cells became malignantly transformed and ultimately contributed to the primary tumour. Some of those cells may have inactivated *p16* function by promoter hypermethylation and contributed to the majority of the primary tumour, while other cells had a 17 bp deletion and made only a minor contribution to the population of primary tumour cells. However, this minor population continued its independent evolution and acquired the ability to create the metastatic tumour in the cervical lymph node.

An alternative interpretation of the data relies on the potential plasticity of DNA methylation. Although DNA methylation can act as a loss of function mutation similar to point mutations or deletions, a significant difference is that while genetic mutations are permanent, hypermethylation of a CpG island may be reversible. An excellent example of how such a scenario may be advantageous to tumour development has been proposed for the E-cadherin gene (*CDH1*).[37] *CDH1* is involved in homotypic cell-cell adhesion of differentiated epithelial cells, and loss of expression has been linked to invasiveness. It is advantageous for a cell to express *CDH1* when growing in a tumour mass, but in order to become invasive, or to leave the tumour mass for metastatic spread, it is advantageous to block expression. Graff *et al*[37] have shown that the prostate cancer cell line TSUPr1 shows moderate levels of hypermethylation of the *CDH1* locus. When this cell line is put into a model culture system for basement membrane invasion, the invasive cells show higher levels of hypermethylation. However, when this cell line is put into a culture model system for three dimensional tumour growth, the cells showed low levels of hypermethylation.[37] This potential for dynamic hypermethylation of promoters affords the opportunity to up- or downregulate gene expression either randomly or in response to other signals. This represents a significant difference between epigenetic and genetic changes.

The lack of hypermethylation seen in the metastatic HNSCC tumours at loci that were previously methylated in the primary tumours may in part be explained by dynamic loss of hypermethylation. This idea, and the idea of the independent development of subpopulations of cells with unique hypermethylation patterns within the primary tumour, is not mutually exclusive. Our findings show that the patterns of CpG island hypermethylation in primary and metastatic HNSCC are complex and suggest that the relationship between those patterns in any one patient may require a more sophisticated explanation than a simple accumulation of changes.

ACKNOWLEDGEMENTS

We would like to thank Fred Wright, William Lemon, and Bin Li for help with statistical analysis, and the Ohio State GSU for DNA sequencing. This work was supported in part by two grants from the NIDCR, DE13123-02 (CP) and DE12704 (JCL). DJS and LJR were supported in part by the T32 CA09338-20 Oncology Training Grant from the National Cancer Institute.

Authors' affiliations

D J Smiraglia, L T Smith, L J Rush, Z Dai, C Plass, Division of Human Cancer Genetics, Department of Molecular Virology, Immunology and Medical Genetics, and Comprehensive Cancer Center, The Ohio State University, Columbus, Ohio 43210, USA
J C Lang, D E Schuller, Department of Otolaryngology, and Comprehensive Cancer Center, The Ohio State University, Columbus, Ohio 43210, USA
L J Rush, Department of Veterinary Biosciences, The Ohio State University, Columbus, Ohio 43210, USA
Z Dai, Department of Pathology, and Comprehensive Cancer Center, The Ohio State University, Columbus, Ohio 43210, USA

REFERENCES

1 **Vokes EE**, Weichselbaum RR, Lippman SM, Hong WK. Head and neck cancer. *N Engl J Med* 1993;**328**:184-94.
2 **Hiratsuka H**, Miyakawa A, Nakamori K, Kido Y, Sunakawa H, Kohama G. Multivariate analysis of occult lymph node metastasis as a prognostic indicator for patients with squamous cell carcinoma of the oral cavity. *Cancer* 1997;**80**:351-6.
3 **Fearon ER**, Vogelstein B. A genetic model for colorectal tumorigenesis. *Cell* 1990;**61**:759-67.
4 **Califano J**, van der Riet P, Westra W, Nawroz H, Clayman G, Piantadosi S, Corio R, Lee D, Greenberg B, Koch W, Sidransky D. Genetic progression model for head and neck cancer: implications for field cancerization. *Cancer Res* 1996;**56**:2488-92.
5 **Sun PC**, Schmidt AP, Pashia ME, Sunwoo JB, Scholnick SB. Homozygous deletions define a region of 8p23.2 containing a putative tumor suppressor gene. *Genomics* 1999;**62**:184-8.
6 **Takebayashi S**, Ogawa T, Jung KY, Muallem A, Mineta H, Fisher SG, Grenman R, Carey TE. Identification of new minimally lost regions on 18q in head and neck squamous cell carcinoma. *Cancer Res* 2000;**60**:3397-403.
7 **Frank CJ**, McClatchey KD, Devaney KO, Carey TE. Evidence that loss of chromosome 18q is associated with tumor progression. *Cancer Res* 1997;**57**:824-7.
8 **Ogawara K**, Miyakawa A, Shiba M, Uzawa K, Watanabe T, Wang XL, Sato T, Kubosawa H, Kondo Y, Tanzawa H. Allelic loss of chromosome 13q14.3 in human oral cancer: correlation with lymph node metastasis. *Int J Cancer* 1998;**79**:312-17.
9 **Pande P**, Mathur M, Shukla NK, Ralhan R. Ets-1: a plausible marker of invasive potential and lymph node metastasis in human oral squamous cell carcinomas. *J Pathol* 1999;**189**:40-5.
10 **Smiraglia DJ**, Plass C. The study of aberrant methylation in cancer via restriction landmark genomic scanning. *Oncogene* 2002;**21**:5414-26.
11 **Rush LJ**, Dai Z, Smiraglia DJ, Gao X, Wright FA, Fruhwald M, Costello JF, Held WA, Yu L, Krahe R, Kolitz JE, Bloomfield CD, Caligiuri MA, Plass C. Novel methylation targets in de novo acute myeloid leukemia with prevalence of chromosome 11 loci. *Blood* 2001;**97**:3226-33.
12 **Fruhwald MC**, O'Dorisio MS, Dai Z, Tanner SM, Balster DA, Gao X, Wright FA, Plass C. Aberrant promoter methylation of previously

unidentified target genes is a common abnormality in medulloblastomas - implications for tumor biology and potential clinical utility. *Oncogene* 2001;**20**:5033-42.
13 **Costello JF**, Fruhwald MC, Smiraglia DJ, Rush LJ, Robertson GP, Gao X, Wright FA, Feramisco JD, Peltomaki P, Lang JC, Schuller DE, Yu L, Bloomfield CD, Caligiuri MA, Yates A, Nishikawa R, Su Huang H, Petrelli NJ, Zhang X, O'Dorisio MS, Held WA, Cavenee WK, Plass C. Aberrant CpG-island methylation has non-random and tumour-type-specific patterns. *Nat Genet* 2000;**24**:132-8.
14 **Costello JF**, Plass C. Methylation matters. *J Med Genet* 2001;**38**:285-303.
15 **Baylin SB**, Herman JG, Graff JR, Vertino PM, Issa JP. Alterations in DNA methylation: a fundamental aspect of neoplasia. *Adv Cancer Res* 1998;**72**:141-96.
16 **Nan X**, Ng HH, Johnson CA, Laherty CD, Turner BM, Eisenman RN, Bird A. Transcriptional repression by the methyl-CpG-binding protein MeCP2 involves a histone deacetylase complex. *Nature* 1998;**393**:386-9.
17 **Ng HH**, Bird A. DNA methylation and chromatin modification. *Curr Opin Genet Dev* 1999;**9**:158-63.
18 **Nan X**, Campoy FJ, Bird A. MeCP2 is a transcriptional repressor with abundant binding sites in genomic chromatin. *Cell* 1997;**88**:471-81.
19 **Bird AP**, Wolffe AP. Methylation-induced repression - belts, braces, and chromatin. *Cell* 1999;**99**:451-4.
20 **Reed AL**, Califano J, Cairns P, Westra WH, Jones RM, Koch W, Ahrendt S, Eby Y, Sewell D, Nawroz H, Bartek J, Sidransky D. High frequency of p16 (CDKN2/MTS-1/INK4A) inactivation in head and neck squamous cell carcinoma. *Cancer Res* 1996;**56**:3630-3.
21 **Akanuma D**, Uzawa N, Yoshida MA, Negishi A, Amagasa T, Ikeuchi T. Inactivation patterns of the p16 (INK4a) gene in oral squamous cell carcinoma cell lines. *Oral Oncol* 1999;**35**:476-83.
22 **Bazan V**, Zanna I, Migliavacca M, Sanz-Casla MT, Maestro ML, Corsale S, Macaluso M, Dardanoni G, Restivo S, Quintela PL, Bernaldez R, Salerno S, Morello V, Tomasino RM, Gebbia N, Russo A. Prognostic significance of p16INK4a alterations and 9p21 loss of heterozygosity in locally advanced laryngeal squamous cell carcinoma. *J Cell Physiol* 2002;**192**:286-93.
23 **Esteller M**, Corn PG, Baylin SB, Herman JG. A gene hypermethylation profile of human cancer. *Cancer Res* 2001;**61**:3225-9.
24 **Hasegawa M**, Nelson HH, Peters E, Ringstrom E, Posner M, Kelsey KT. Patterns of gene promoter methylation in squamous cell cancer of the head and neck. *Oncogene* 2002;**21**:4231-6.
25 **Riese U**, Dahse R, Fiedler W, Theuer C, Koscielny S, Ernst G, Beleites E, Claussen U, von Eggeling F. Tumor suppressor gene p16 (CDKN2A) mutation status and promoter inactivation in head and neck cancer. *Int J Mol Med* 1999;**4**:61-5.
26 **Rosas SL**, Koch W, da Costa Carvalho MG, Wu L, Califano J, Westra W, Jen J, Sidransky D. Promoter hypermethylation patterns of p16, O6-methylguanine-DNA-methyltransferase, and death-associated protein kinase in tumors and saliva of head and neck cancer patients. *Cancer Res* 2001;**61**:939-42.
27 **Sanchez-Cespedes M**, Esteller M, Wu L, Nawroz-Danish H, Yoo GH, Koch WM, Jen J, Herman JG, Sidransky D. Gene promoter hypermethylation in tumors and serum of head and neck cancer patients. *Cancer Res* 2000;**60**:892-5.
28 **Fruhwald MC**, O'Dorisio MS, Dai Z, Rush LJ, Krahe R, Smiraglia DJ, Pietsch T, Elsea SH, Plass C. Aberrant hypermethylation of the major breakpoint cluster region in 17p11.2 in medulloblastomas but not supratentorial PNETs. *Genes Chrom Cancer* 2001;**30**:38-47.
29 **Okazaki Y**, Okuizumi H, Sasaki N, Ohsumi T, Kuromitsu J, Hirota N, Muramatsu M, Hayashizaki Y. An expanded system of restriction landmark genomic scanning (RLGS Ver 1.8). *Electrophoresis* 1995;**16**:197-202.
30 **Watanabe S**, Kawai J, Hirotsune S, Suzuki H, Hirose K, Taga C, Ozawa N, Fushiki S, Hayashizaki Y. Accessibility to tissue-specific genes from methylation profiles of mouse brain genomic DNA. *Electrophoresis* 1995;**16**:218-26.
31 **Smiraglia DJ**, Frühwald MC, Costello JF, McCormick SP, Dai Z, Peltomäki P, O'Dorisio MS, Cavenee WK, Plass C. A new tool for the rapid cloning of amplified and hypermethylated human DNA sequences from restriction landmark genome scanning gels. *Genomics* 1999;**58**:254-62.
32 **Herman JG**, Graff JR, Myohanen S, Nelkin BD, Baylin SB. Methylation-specific PCR: a novel PCR assay for methylation status of CpG islands. *Proc Natl Acad Sci USA* 1996;**93**:9821-6.
33 **Gramza AW**, Lucas JM, Mountain RE, Schuller DE, Lang JC. Efficient method for preparing normal and tumor tissue for RNA extraction. *Biotechniques* 1995;**18**:228-31.
34 **Plass C**, Weichenhan D, Catanese J, Costello JF, Yu F, Yu L, Smiraglia D, Cavenee WK, Caligiuri MA, deJong P, Held WA. An arrayed human not I-EcoRV boundary library as a tool for RLGS spot analysis. *DNA Res* 1997;**4**:253-5.
35 **Gardiner-Garden M**, Frommer M. CpG islands in vertebrate genomes. *J Mol Biol* 1987;**196**:261-82.
36 **Warnecke PM**, Stirzaker C, Melki JR, Millar DS, Paul CL, Clark SJ. Detection and measurement of PCR bias in quantitative methylation analysis of bisulphite-treated DNA. *Nucleic Acids Res* 1997;**25**:4422-6.
37 **Graff JR**, Gabrielson E, Fujii H, Baylin SB, Herman JG. Methylation patterns of the E-cadherin 5′ CpG island are unstable and reflect the dynamic, heterogeneous loss of E-cadherin expression during metastatic progression. *J Biol Chem* 2000;**275**:2727-32.